Optimal Beamforming and Outage Analysis for Max Mean SNR under RIS-aided Communication

Kali Krishna Kota, Praful D. Mankar, Harpreet S. Dhillon

***Abstract*—This paper investigates beamforming for a reconfigurable intelligent surface (RIS)-aided multiple input single output (MISO) communication system in the presence of Rician multipath fading. Our objective is to jointly optimize the transmit beamformer and RIS phase shift matrix that maximizes the mean signal-to-noise ratio (SNR) of the signal received over direct and indirect links. While numerical approaches have been known to address such optimization problems, our work distinguishes itself by providing closed-form expressions for the optimal transmit beamformer and RIS phase shifter. In particular, we maximize a carefully constructed lower bound on the mean SNR, which is more conducive to analytical treatment. Additionally, we establish that the effective channel envelope, under optimal beamforming, follows the Rice distribution. We leverage this result to derive a closed-form expression for outage probability within the proposed beamforming framework, which is subsequently employed to derive an analytical expression for ergodic capacity. Finally, we numerically validate the effectiveness of our proposed beamforming closed-form solution by demonstrating that it performs very close to the algorithmically obtained optimal solution that maximizes the exact mean SNR.**

***Index Terms*—RIS, Optimal Beamforming, Rician Channel, Outage Analysis, Ergodic Capacity, and Maximum Mean SNR.**

I. Introduction

Reconfigurable Intelligent Surface (RIS) is an upcoming physical layer technology that is being considered to play an important role in the development of the sixth generation of communication standards because of its many advantages, such as high data rate and enhanced coverage [2]. In essence, RIS is a planar array consisting of numerous sub-wavelength-sized elements made of meta-materials. These elements are individually configured to induce a phase shift on the impinging electromagnetic wave (EM), effectively changing the direction of the reflected EM wave. This capability enables the partial control of the local propagation environment [3]. Consequently, it has the potential to influence key characteristics of the propagation environment, such as reflection, refraction, and scattering, which were thus far assumed to be uncontrollable in wireless communications systems [4]. If configured properly, RISs can reduce the effect of fading by redirecting the impinging signals such that they add constructively at the receiver. Even though the idea of using RIS is conceptually similar to several well-studied technologies, such as relay transmission, backscatter communication, and massive multiple input multiple output (MIMO), a key differentiating feature is its low-cost implementation and lower power consumption, especially when all the elements are passive (which will be our assumption in this paper). Additionally, RISs operate in full-duplex mode by design without additional hardware requirements, which is not the case in the competing technologies mentioned above [5].

Needless to say, including RIS in communication systems comes with its own challenges. Two particularly important ones are 1) channel estimation and 2) joint design of transmit beamformer and RIS phase shift matrix. The challenges in channel estimation stem from the high dimensionality of the channel matrix [6] and the lack of active elements in passive RISs for aiding the channel estimation process [7]. Therefore, it is not always reasonable to assume perfect channel state information (CSI) at the transmitter for optimal beamforming. Moreover, instantaneous CSI feedback and RIS reconfiguration will increase the system overhead significantly and also require complex RIS design for quick reconfigurability. *Due to these reasons, it is more practical to assume the statistical knowledge of CSI for optimal beamforming for RIS-aided communications systems, which is the main theme of this paper.*

Related Works: The authors of [8]–[10] investigate the joint optimal instantaneous transmit beamformer and phase shift matrix design for RIS-aided communication systems while assuming perfect CSI at the transmitter. Authors in [8], [9] propose iterative algorithms such as fixed point iteration, manifold optimization, and branch-and-bound techniques to maximize the signal-to-noise ratio (SNR). Further, [10] proposes a new sum-path-gain maximization criterion to obtain a suboptimal solution, which is numerically shown to achieve near-optimal RIS-MIMO channel capacity. While these works provided useful design insights, they all considered instantaneous CSI knowledge at the transmitter, which is not always feasible and practical. Inspired by this, [11]–[14] aim to jointly optimize the transmit beamformers and phase shifter using statistical CSI. The authors in [11] maximize the sum rate for a multi-user MIMO system in the presence of spatial correlation. The authors of [12] and [13] derive closed-form approximate expressions for the sum rate and maximize it with respect to the transmit beamformer and RIS phase shifts in downlink and uplink, respectively. A fractional programming-based iterative solution is presented in [12], whereas [13] proposes a genetic algorithm-based solution. Finally, [14] presents an optimal solution that maximizes the mean SNR, or equivalently the upper bound on ergodic capacity, for the RIS-aided MISO system.

K.K. Kota and P. D. Mankar are with SPCRC, IIIT Hyderabad, India (Email: kali.kota@research.iiit.ac.in, praful.mankar@iiit.ac.in). H. S. Dhillon is with Wireless@VT, Department of ECE, Virginia Tech, Blacksburg, VA (Email: hdhillon@vt.edu). H. S. Dhillon gratefully acknowledges the support of US NSF (grant ECCS-2030215).
The preprint of this paper is available on arXiv (2211.09337), and the expanded journal version of this work is available at [1].

The solutions are obtained by alternating over the transmit beamformer and phase shift matrix sub-problems for which closed-form expressions are obtained. However, such numerical solutions often prohibit further analytical investigation, such as the understanding of the exact functional dependence of the optimal solutions on key system parameters. *Therefore, it is equally, or perhaps even more, important to obtain optimal solutions in closed form, which will be our objective.*

It is worth noting that the statistical CSI-based design of RIS-aided systems not only circumvents the system design complexity issue but often makes the analysis tractable while resulting in comparable performance to the instantaneous CSI-based beamforming. The performance of the beamformer scheme is usually characterized using the outage analysis. Along these lines, the authors of [15], [16] analyze the outage performance for RIS-aided communication systems. The authors of [15] derive a closed-form expression for the asymptotic outage probability, whereas [16] obtain an approximate channel gain distributions for two cases: 1) RIS-aided system and 2) RIS-at-transmitter system. However, it is important to emphasize that all the works proposing closed-form expressions for performance analysis have considered a single input single output (SISO) setup. This might be attributed to the fact that the beamforming scheme performance analysis becomes intractable for more realistic settings including multi-antenna, line of sight (LoS) components, presence of direct link, etc., especially when the solution is algorithmic in nature. *This paper focuses on optimal beamforming and characterization of its performance for RIS-aided MISO system in the presence of LoS components and multipath fading along both the direct and indirect links.*

Contributions: In this paper, we consider an RIS-aided MISO system where the transmitter performs optimal beamforming based on the statistical knowledge of CSI. Moreover, we consider a general setup by assuming the presence of LoS and multipath fading along direct and indirect links. Our main technical contribution is deriving closed-form expressions for the joint optimal transmit beamformer and RIS phase shift matrix problem by maximizing a carefully constructed lower-bound on the mean SNR. For the derived optimal solution, we also show that the channel envelope is Rice-distributed, resulting in an accurate closed-form expression for the outage probability and an analytical expression for the ergodic capacity. Using numerical comparisons, we demonstrate that the proposed beamforming method provides a tight lower bound on the ergodic capability and a tight upper bound on the outage probability.

Notations: The notations a^* and $|a|$ represent the conjugate and absolute value of a. $\|\mathbf{a}\|$ is the norm of vector $\mathbf{a}$, whereas $\mathbf{A}^T$, $\mathbf{A}^H$, $\mathbf{A}_{i,:}$, $\mathbf{A}_{:,i}$ and $\{\mathbf{A}\}_{ij}$ are the transpose, Hermitian, i-th row, i-th column and ij-th element of the matrix $\mathbf{A}$, respectively. The notation $\mathbb{C}^{M\times N}$ is the set of $M\times N$ complex matrices and $\mathrm{I_M}$ is $M\times M$ identity matrix. $\mathbb{E}[\cdot]$ is the statistical expectation operator and $\mathcal{CN}(\mu,\mathbf{K})$ denotes complex circular Gaussian distribution with mean μ and covariance matrix $\mathbf{K}$.

II. System Model

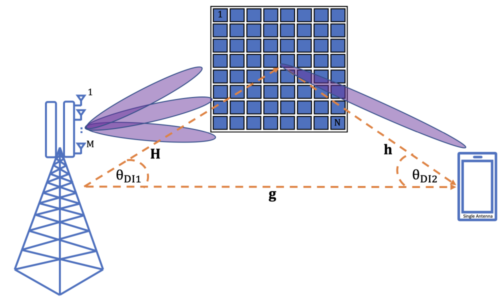

Figure 1. Illustration of RIS-aided MISO Downlink System

This paper considers a RIS-assisted MISO communication system consisting of a transmitter equipped with M antennas, RIS with N elements, and a single antenna receiver. We assume that the transmitted signal reaches the receiver through two links: 1) the direct link from the transmitter and 2) the indirect link through RIS. We also consider the presence of Line-of-Sight (LoS) components in both links. Furthermore, the transmitter is assumed to possess knowledge of these components, using it to determine the optimal transmit beamformer and the RIS phase shift matrix. To model multipath fading for this scenario, we consider Rician fading with factor K.

The direct link channel coefficient is modeled as

$$\mathbf{g} = \kappa_{\mathrm{l}}\bar{\mathbf{g}} + \kappa_{\mathrm{n}}\tilde{\mathbf{g}}, \tag{1}$$

where $\kappa_{\mathrm{l}} = \sqrt{\frac{K}{1+K}}$, $\kappa_{\mathrm{n}} = \sqrt{\frac{1}{1+K}}$, $\tilde{\mathbf{g}} \sim \mathcal{CN}(0,\mathrm{I_M})$, $\bar{\mathbf{g}} = a_M(\theta_{\mathrm{DD}})$, and θ_{DD} is the departure angle of the direct link. Here, $a_M(\theta)$ is a response vector and is given by

$$a_M(\theta) = [1,\ e^{j2\pi\frac{d}{\lambda}\sin(\theta)},\ \ \ldots\ \ ,\ e^{j2\pi(M-1)\frac{d}{\lambda}\sin(\theta)}]^T,$$

where λ is the operating wavelength and d is the antenna separation distance. Similarly, the channel coefficients for transmitter-RIS and RIS-receiver links are modeled as

$$\mathbf{H} = \kappa_{\mathrm{l}}\bar{\mathbf{H}} + \kappa_{\mathrm{n}}\tilde{\mathbf{H}} \ \text{ and } \ \mathbf{h} = \kappa_{\mathrm{l}}\bar{\mathbf{h}} + \kappa_{\mathrm{n}}\tilde{\mathbf{h}}, \tag{2}$$

respectively, where $\bar{\mathbf{h}} = a_N(\theta_{\mathrm{DI_2}})$ and $\bar{\mathbf{H}} = a_N(\theta_{\mathrm{AI_1}})a_M^T(\theta_{\mathrm{DI_1}})$ such that $\theta_{\mathrm{DI_1}}$ and $\theta_{\mathrm{DI_2}}$ are the departure angles from the transmitter and RIS, respectively, and $\theta_{\mathrm{AI_1}}$ is the arrival angle at the RIS. Also, $\tilde{\mathbf{h}} \sim \mathcal{CN}(0,\mathrm{I_N})$ and $\tilde{\mathbf{H}}_{:,i} \sim \mathcal{CN}(0,\mathrm{I_N})$.

Let $\mathbf{f} \in \mathbb{C}^M$ and $\boldsymbol{\psi} \in \mathbb{C}^N$ be the transmit beamforming vector and the RIS phase shift vector, respectively with $\boldsymbol{\Phi} = \mathrm{diag}(\boldsymbol{\psi})$ be the RIS phase shift matrix. The elements of $\boldsymbol{\psi}$ are unit magnitude as RIS is considered to be passive. Considering the far-field propagation scenario [17], the path loss for the direct and indirect links are modeled as $d_o^{-\alpha}$ and $(d_1d_2)^{-\alpha}$, respectively, where α is the path loss exponent and d_o, d_1, and d_2 are the link distances of the transmitter-receiver, transmitter-RIS, and RIS-receiver links, respectively.

The signal received at a given time can be written as

$$y = (d_1d_2)^{-\frac{\alpha}{2}}\mathbf{h}^T\boldsymbol{\Phi}\mathbf{H}\mathbf{f}x + d_o^{-\frac{\alpha}{2}}\mathbf{g}^T\mathbf{f}x + w, \tag{3}$$

where x is the transmitted symbol with transmit power $\mathbb{E}[xx^H] = P_s$ and $w \sim \mathcal{CN}(0,\sigma_w^2)$. Thus, the SNR becomes

$$\mathrm{SNR} = \gamma|\mathbf{h}^T\boldsymbol{\Phi}\mathbf{H}\mathbf{f} + \mu\mathbf{g}^T\mathbf{f}|^2, \tag{4}$$

where $\gamma = (d_1 d_2)^{-\alpha}\frac{P_s}{\sigma_w^2}$ and $\mu = \left(\frac{d_0}{d_1 d_2}\right)^{-\frac{\alpha}{2}}$.

The ergodic capacity is obtained as

$$\mathrm{EC} = \mathbb{E}[\log_2(1+\mathrm{SNR})]. \tag{5}$$

Our objective is to maximize the ergodic capacity with respect to RIS phase shift matrix $\mathbf{\Phi}$ and transmit beamforming vector $\mathbf{f}$. However, (5) is mathematically intractable, making it difficult to solve directly. Thus we use Jensen's inequality to obtain an upper bound on the capacity, i.e., $\mathrm{EC} \leq \log_2(1+\mathbb{E}[\mathrm{SNR}])$, and maximize it. This is equivalent to maximizing $\mathbb{E}[\mathrm{SNR}]$, which we refer to as the *Max mean SNR scheme* throughout the paper. Now, using (4), we formulate the optimization problem as

$$\max_{\mathbf{f},\boldsymbol{\psi}} \quad \gamma\mathbb{E}[|\mathbf{h}^T\mathbf{\Phi}\mathbf{H}\mathbf{f} + \mu\mathbf{g}^T\mathbf{f}|^2], \tag{6a}$$

$$\text{s.t.} \quad \|\mathbf{f}\|^2 = 1, \tag{6b}$$

$$|\boldsymbol{\psi}_k| = 1, \quad \forall k = 0,\dots,N-1, \tag{6c}$$

where (6b) is the unit norm constraint of the transmit beamformer and (6c) is the unit magnitude constraint on the passive RIS elements. To characterize the performance of the statistical CSI-based maximization of mean SNR scheme, we analyze its *outage probability* which is defined as the probability that the instantaneous SNR with optimal $\mathbf{f}$ and $\mathbf{\Phi}$ is below threshold β and is given as

$$\mathrm{P}_{\mathrm{out}}(\beta) = \mathbb{P}[\mathrm{SNR} \leq \beta]. \tag{7}$$

Further, we also characterize the ergodic capacity given in (5) that is achievable with the statistically optimal $\mathbf{f}$ and $\mathbf{\Phi}$.

III. Optimal Beamforming and Outage Analysis

In this section, we present our two main contributions: 1) the joint optimization of the statistical-CSI-based beamformer and phase shift matrix and 2) the outage and capacity analyses. The optimization problem (6) that maximizes $\mathbb{E}[\mathrm{SNR}]$ is non-convex due to the coupled beamformer and phase shift matrix variables. So, deriving a closed-form solution for this objective is challenging. Hence, we construct a lower bound on $\mathbb{E}[\mathrm{SNR}]$ that is more conducive to analytical treatment and facilitates the derivation of the optimal beamformer and phase shift matrix in closed form, as discussed next.

A. Statistical CSI-based Beamforming

In this subsection, we obtain the optimal transmit beamformer and RIS phase shift matrix that maximizes (6). $\mathbb{E}[\mathrm{SNR}]$ is further simplified and is obtained in [14, Appendix A] as

$$\mathbb{E}[\mathrm{SNR}] = \gamma|\kappa_l^2\bar{\mathbf{h}}^T\mathbf{\Phi}\bar{\mathbf{H}}\mathbf{f} + \mu\kappa_l\bar{\mathbf{g}}^T\mathbf{f}|^2 + \gamma\kappa_l^2\kappa_n^2\|\bar{\mathbf{H}}\mathbf{f}\|^2 + \gamma(\kappa_l^2\kappa_n^2 + \kappa_n^4)N + \gamma\mu^2\kappa_n^2.$$

Thus, we can rewrite the optimization problem (6) as

$$\max_{\mathbf{f},\boldsymbol{\psi}} \quad |\kappa_l^2\bar{\mathbf{h}}^T\mathbf{\Phi}\bar{\mathbf{H}}\mathbf{f} + \mu\kappa_l\bar{\mathbf{g}}^T\mathbf{f}|^2 + \kappa_l^2\kappa_n^2\|\bar{\mathbf{H}}\mathbf{f}\|^2, \tag{8a}$$

$$\text{s.t.} \quad \|\mathbf{f}\|^2 = 1, \tag{8b}$$

$$|\boldsymbol{\psi}_k| = 1, \quad \forall k = 0,\dots,N-1. \tag{8c}$$

The above problem can be solved using techniques such as alternating optimization [14]. However, such numerical solutions do not provide insights into the exact functional dependence of the optimal solution on the key system parameters. Therefore, closed-form expressions for $\mathbf{f}$ and $\boldsymbol{\psi}$ are desirable. Towards this goal, we first obtain the optimal $\boldsymbol{\psi}$ for a given $\mathbf{f}$ in III-A1. Using this optimal $\boldsymbol{\psi}$ solution, we modify the objective function (8a) and solve for optimal $\mathbf{f}$ in III-A2.

1) Optimal RIS Phase Shift Matrix:

For a given $\mathbf{f}$, the optimization problem for the RIS phase shift matrix is

$$\max_{\boldsymbol{\psi}} \quad |\kappa_l^2\boldsymbol{\psi}^T\mathrm{diag}(\bar{\mathbf{h}})\bar{\mathbf{H}}\mathbf{f} + \mu\kappa_l\bar{\mathbf{g}}^T\mathbf{f}|^2, \tag{9a}$$

$$\text{s.t.} \quad |\boldsymbol{\psi}_k| = 1, \quad \forall k = 0,\cdots,N-1, \tag{9b}$$

where $\bar{\mathbf{h}}^T\mathbf{\Phi} = \boldsymbol{\psi}^T\mathrm{diag}(\bar{\mathbf{h}})$. To solve (9), the objective (9a) is upper-bounded using the triangle inequality as

$$|\kappa_l^2\boldsymbol{\psi}^T\mathrm{diag}(\bar{\mathbf{h}})\bar{\mathbf{H}}\mathbf{f} + \mu\kappa_l\bar{\mathbf{g}}^T\mathbf{f}| \leq |\kappa_l^2\boldsymbol{\psi}^T\mathrm{diag}(\bar{\mathbf{h}})\bar{\mathbf{H}}\mathbf{f}| + |\mu\kappa_l\bar{\mathbf{g}}^T\mathbf{f}|, \tag{10}$$

where the equality holds when $\boldsymbol{\psi}^T\mathrm{diag}(\bar{\mathbf{h}})\bar{\mathbf{H}}\mathbf{f} = c\bar{\mathbf{g}}^T\mathbf{f}$ for a constant c. To achieve equality, we set

$$\boldsymbol{\psi}^T = c\bar{\mathbf{g}}^T\mathbf{f}\mathbf{w}, \tag{11}$$

where $\mathbf{w} = \mathbf{f}^H\mathbf{E}^H/\|\mathbf{E}\mathbf{f}\|^2$ is the pseudoinverse of $\mathbf{E}\mathbf{f}$ and $\mathbf{E} = \mathrm{diag}(\bar{\mathbf{h}})\bar{\mathbf{H}}$. Nonetheless, the constraint in (9b) also must be satisfied. Towards this, we observe the elements of $\mathbf{w}$ to have equal magnitudes and thus we set c to ensure (9b) as follows. Let $\mathbf{e}_n = \mathbf{E}_{n,:}$, and by using $\bar{\mathbf{h}}$ and $\bar{\mathbf{H}}$, we show that

$$\{\mathbf{e}_n^H\mathbf{e}_n\}_{i,k} = \begin{cases} 1, & \text{if } i = k, \\ e^{j2\pi(i-k)\frac{d}{\lambda}\sin(\theta_{\mathrm{DI}_1})}, & \text{if } i \neq k. \end{cases}$$

This results in $\mathbf{f}^H\mathbf{e}_n^H\mathbf{e}_n\mathbf{f} = \mathbf{f}^H\mathbf{e}_m^H\mathbf{e}_m\mathbf{f}$, which further implies

$$\|\mathbf{e}_n\mathbf{f}\|^2 = \|\mathbf{e}_m\mathbf{f}\|^2. \tag{12}$$

Additionally, we also observe that

$$\|\mathbf{E}\mathbf{f}\|^2 = \sum_{n=0}^{N-1}|\mathbf{e}_n\mathbf{f}|^2 = N|\mathbf{e}_n\mathbf{f}|^2. \tag{13}$$

Thus, by using (12) and (13), we obtain the absolute value of the k-th element of RHS of (11) as

$$|\bar{\mathbf{g}}^T\mathbf{f}\mathbf{w}_k| = \frac{|\bar{\mathbf{g}}^T\mathbf{f}|}{N|\mathbf{e}_n\mathbf{f}|}, \forall k = 1,\cdots N$$

where $|\mathbf{w}_k| = \frac{1}{N|\mathbf{e}_n\mathbf{f}|}$; $\forall k$. Finally, by substituting the above equation in (11), we obtain the optimal RIS phase shift vector with unit magnitude elements as

$$\boldsymbol{\psi}^{\star T} = \frac{N|\mathbf{e}_n\mathbf{f}|}{|\bar{\mathbf{g}}^T\mathbf{f}|}\bar{\mathbf{g}}^T\mathbf{f}\mathbf{w}. \tag{14}$$

2) Optimal Transmit Beamforming

The optimization problem for the *Max mean SNR scheme* to obtain the optimal transmit beamformer for the optimal $\boldsymbol{\psi}^\star$ is

$$\max_{\mathbf{f}} \quad |\kappa_l^2\boldsymbol{\psi}^{\star T}\mathrm{diag}(\bar{\mathbf{h}})\bar{\mathbf{H}}\mathbf{f} + \mu\kappa_l\bar{\mathbf{g}}^T\mathbf{f}|^2 + \kappa_l^2\kappa_n^2\|\bar{\mathbf{H}}\mathbf{f}\|^2, \tag{15a}$$

$$\text{s.t.} \quad \|\mathbf{f}\|^2 = 1. \tag{15b}$$

To obtain the closed-form solution we begin by substituting $\boldsymbol{\psi}^\star$ in the first term of (15a) as

$$\begin{aligned} &|\kappa_l^2\boldsymbol{\psi}^{\star T}\mathbf{E}\mathbf{f} + \mu\kappa_l\bar{\mathbf{g}}^T\mathbf{f}|^2 \\ &= \kappa_l^4|\boldsymbol{\psi}^{\star T}\mathbf{E}\mathbf{f}|^2 + \mu^2\kappa_l^2|\bar{\mathbf{g}}^T\mathbf{f}|^2 + 2\kappa_l^3\mu|\boldsymbol{\psi}^{\star T}\mathbf{E}\mathbf{f}||\bar{\mathbf{g}}^T\mathbf{f}|, \\ &= N^2\kappa_l^4|\mathbf{e}_n\mathbf{f}|^2 + \mu^2\kappa_l^2|\bar{\mathbf{g}}^T\mathbf{f}|^2 + 2N\kappa_l^3\mu|\mathbf{e}_n\mathbf{f}||\bar{\mathbf{g}}^T\mathbf{f}|, \end{aligned} \tag{16}$$

where $\mathbf{wEf} = 1$ follows from (11). Next, the second term of (15a) is simplified as

$$\begin{aligned} \|\bar{\mathbf{H}}\mathbf{f}\|^2 &= \mathbf{f}^H\bar{\mathbf{H}}^H\bar{\mathbf{H}}\mathbf{f}, \\ &\overset{(a)}{=} \mathbf{f}^H\bar{\mathbf{H}}^H\mathrm{diag}(\bar{\mathbf{h}})^H\mathrm{diag}(\bar{\mathbf{h}})\bar{\mathbf{H}}\mathbf{f}, \\ &= \mathbf{f}^H\mathbf{E}^H\mathbf{E}\mathbf{f}, \\ &\overset{(b)}{=} N|\mathbf{e}_n\mathbf{f}|^2, \end{aligned} \tag{17}$$

where steps (a) and (b) follow from $\mathrm{diag}(\bar{\mathbf{h}})^H\mathrm{diag}(\bar{\mathbf{h}}) = \mathbf{I}_\mathrm{N}$ and (13), respectively. Now, combining (16) and (17), (15a) becomes

$$\begin{aligned} |\kappa_l^2\boldsymbol{\psi}^{\star T}\mathrm{diag}(\bar{\mathbf{h}})\bar{\mathbf{H}}\mathbf{f} + \mu\kappa_l\bar{\mathbf{g}}^T\mathbf{f}|^2 + \kappa_l^2\kappa_n^2\|\bar{\mathbf{H}}\mathbf{f}\|^2 \\ = w_1|\mathbf{e}_n\mathbf{f}|^2 + w_2|\bar{\mathbf{g}}^T\mathbf{f}|^2 + w_3|\mathbf{e}_n\mathbf{f}||\bar{\mathbf{g}}^T\mathbf{f}|, \\ = w_1\mathbf{f}^H\mathbf{E}_n\mathbf{f} + w_2\mathbf{f}^H\mathbf{G}\mathbf{f} + w_3|\mathbf{f}^H\mathbf{E}_g\mathbf{f}|, \\ \geq \mathbf{f}^H\mathbf{Z}\mathbf{f}, \end{aligned} \tag{18}$$

where $\mathbf{E}_n = \mathbf{e}_n^H\mathbf{e}_n$, $\mathbf{G} = \bar{\mathbf{g}}^*\bar{\mathbf{g}}^T$, $\mathbf{E}_g = \mathbf{e}_n^H\bar{\mathbf{g}}^T$ and $\mathbf{Z} = w_1\mathbf{E}_n + w_2\mathbf{G}$ such that $w_1 = N^2\kappa_l^4 + N\kappa_l^2\kappa_n^2$, $w_2 = \mu^2\kappa_l^2$, and $w_3 = 2N\mu\kappa_l^3$. Here, $\mathbf{Z}$ is a positive definite matrix because $\mathbf{E}_n$ and $\mathbf{G}$ are symmetric matrices. This results in the lower bound (LB) given in (18) become convex in $\mathbf{f}$. Further, it is worth noting that the LB is tight for two reasons: 1) $w_1, w_2 \gg w_3$, and 2) the eigenvalues of $\mathbf{E}_n$ and $\mathbf{G}$ are much larger than the $|\mathbf{f}^H\mathbf{E}_g\mathbf{f}|$ for any given $\mathbf{f}$. Using this, we simplify the optimization problem for maximizing the LB of $\mathbb{E}[\mathrm{SNR}]$, for given $\boldsymbol{\psi}^\star$, as

$$\max_{\mathbf{f}} \quad \mathbf{f}^H\mathbf{Z}\mathbf{f}, \tag{19a}$$

$$\text{s.t.} \quad \|\mathbf{f}\|^2 = 1, \tag{19b}$$

This optimization problem is equivalent to the Rayleigh quotient maximization, whose solution is given by the dominant eigenvector of $\mathbf{Z}$. We summarize the optimal solution for the transmit beamforming vector and the phase shifter matrix in the following theorem.

Theorem 1. *The statistical CSI-based optimal transmit beamformer and RIS phase shift vector that maximizes the LB on* $\mathbb{E}[\mathrm{SNR}]$ *(given in* (19a)*) are*

$$\mathbf{f}^* = \mathbf{v}_1 \quad \textit{and} \quad \boldsymbol{\psi}^\star = \frac{N|\mathbf{e}_n\mathbf{f}^\star|}{|\mathbf{g}^T\mathbf{f}^\star|}\mathbf{w}^T\mathbf{f}^{\star T}\mathbf{g}, \tag{20}$$

respectively, where $\mathbf{v}_1$ *is the principal eigenvector of* $\mathbf{Z}$.

B. Outage and Ergodic Capacity

In this subsection, we analyze outage probability and ergodic capacity for the proposed statistical CSI-based optimal beamformer $\mathbf{f}^\star$ and RIS phase shift matrix $\boldsymbol{\psi}^\star$ obtained in Theorem 1. For the given $\mathbf{f}^\star$ and $\boldsymbol{\psi}^\star$, the instantaneous SNR is

$$\mathrm{SNR} = \gamma|\boldsymbol{\psi}^{\star T}\mathrm{diag}(\mathbf{h})\mathbf{H}\mathbf{f}^\star + \mu\mathbf{g}^T\mathbf{f}^\star|^2.$$

Thus, the outage probability and ergodic capacity become

$$\mathrm{P}_\mathrm{out}(\beta) = \mathbb{P}[|\boldsymbol{\psi}^{\star T}\mathrm{diag}(\mathbf{h})\mathbf{H}\mathbf{f}^\star + \mu\mathbf{g}^T\mathbf{f}^\star| \leq \sqrt{\beta/\gamma}], \tag{21}$$

$$\text{and} \quad \mathrm{EC} = \mathbb{E}[\log_2(1 + \gamma|\boldsymbol{\psi}^{\star T}\mathrm{diag}(\mathbf{h})\mathbf{H}\mathbf{f}^\star + \mu\mathbf{g}^T\mathbf{f}^\star|^2)]. \tag{22}$$

We derive an accurately approximate closed-form expression for this outage probability in Theorem. 2.

Theorem 2. *For the optimal transmit beamformer* $\mathbf{f}^\star$ *and phase shifter* $\boldsymbol{\psi}^\star$ *obtained in Theorem 1, the channel envelope approximately follows a Rice distribution, which gives the outage probability as*

$$\mathrm{P}_\mathrm{out}(\beta) = 1 - Q_1\left(\nu/\sqrt{2}\sigma, \sqrt{\beta/\gamma}/\sqrt{2}\sigma\right), \tag{23}$$

where $Q_1(\cdot)$ *is a Marcum Q-function, and*

$$\nu = N\kappa_l^2|\mathbf{e}_n\mathbf{f}^\star| + \mu\kappa_l|\bar{\mathbf{g}}^T\mathbf{f}^\star|,$$

$$\textit{and} \quad \sigma^2 = N\kappa_n^2(1 + \kappa_l^2|\mathbf{e}_n\mathbf{f}^\star|^2) + \mu^2\kappa_n^2.$$

Proof. Please refer to Appendix A for the proof. □

We now evaluate ergodic capacity given in (22) by using Theorem 2 as done in the following corollary.

Corollary 1. *The ergodic capacity of the optimal transmit beamformer and RIS phase shifter given in Theorem 1 is*

$$\mathrm{EC} = \frac{1}{\ln(2)}\int_0^\infty \frac{1}{1+u}Q_1\left(\frac{\nu}{\sqrt{2}\sigma}, \frac{\sqrt{u/\gamma}}{\sqrt{2}\sigma}\right)\mathrm{d}u. \tag{24}$$

IV. Numerical Results and Discussion

In this section, we present the numerical performance analysis of the proposed beamforming scheme for maximizing the LB of $\mathbb{E}[\mathrm{SNR}]$. We refer to the proposed scheme as *Max LB* $\mathbb{E}[\mathrm{SNR}]$. We also compare the performance of our proposed scheme with the scheme maximizing exact $\mathbb{E}[\mathrm{SNR}]$ using statistical CSI [14] and the scheme maximizing instantaneous SNR using perfect CSI. We refer to the former scheme as *Max* $\mathbb{E}[\mathrm{SNR}]$ and the latter one as *Max SNR*. The parameters γ and μ, defined below (4), represent the received indirect link SNR and the square root of the ratio of received SNRs over direct and indirect links, respectively, observed under the SISO channel. Besides, μ is crucial for optimizing the transmit beamformer, as can be verified using (18) and the discussion below it. To highlight this, we present the numerical results for various system parameters, including γ, μ. For the numerical analysis, we consider $M = 4, N = 32, \theta_\mathrm{DD} = 0, \theta_\mathrm{DI1} = \frac{1}{4}\pi, \theta_\mathrm{DI2} = \frac{8}{5}\pi, K = 5, \alpha = 3.5, \gamma = 0$ dB, and $\mu = 5$ dB; unless mentioned otherwise.

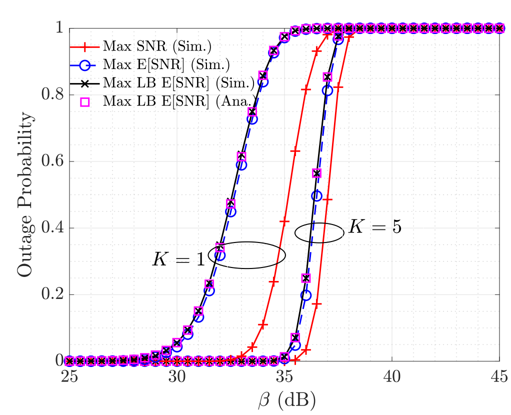

Figure 2. Outage Probability.

Figure 2 presents the outage performance achieved by the proposed scheme, along with a comparison against the above-mentioned beamforming schemes. In our analysis, we first verify that the derived outage probability for the proposed scheme in Theorem 2 matches the simulation. Further, the result indicates that the outage of the proposed *Max LB* $\mathbb{E}[\text{SNR}]$ scheme serves as a tight upper bound to the *Max Mean SNR* scheme. This observation establishes the efficacy of the proposed *Max LB Mean SNR* scheme in solving the original optimization problem. Finally, we compare the outage performance with the benchmark *Max SNR* scheme, where we observe the performance gap reducing with increasing Rice fading factor K, which is also deducible from Fig. 3.

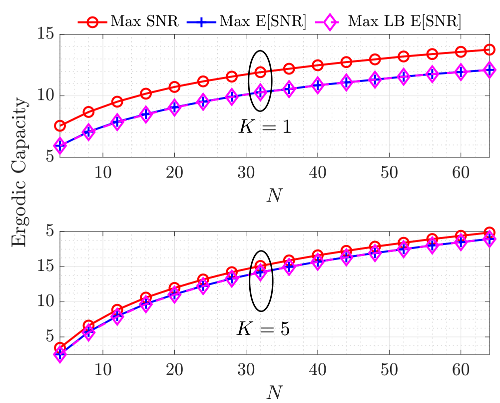

Figure 3. Ergodic capacity vs. number of RIS elements N.

In Fig. 3, we observe the capacity increasing as the number of RIS reflecting elements N increases. The figure further verifies the tightness of the proposed *Max LB Mean SNR* scheme to the capacity achieved via *Max Mean SNR* for various values of N. Finally, we observe that the performance gap between the proposed scheme and the benchmark *Max SNR* reduces with increasing K. This observation is consistent with our earlier observation in the outage analysis.

Next, Fig. 4 presents the impact of μ on the capacity performance. In particular, given γ, increasing μ is equivalent to increasing the SNR of the direct link that, in turn, increases the overall capacity. Additionally, the figure shows the capacity to be increasing as γ increases. This increment is independent of μ as well as other parameters (which can be seen from (22)).

Figure 5 provides insights into the impact of the angular difference between direct and indirect links from the transmitter, denoted as $\theta = \theta_{\text{DI}_1} - \theta_{\text{DD}}$, on the ergodic capacity performance. It can be seen that the capacity decreases from its maximum value at $\theta = 0$ to its minimum value at $\theta = \frac{\pi}{2}$. This is because, as θ increases, the direct and indirect links get spatially separated, making it difficult to form a narrow transmit beam, resulting in lesser array gains. Furthermore, the performance gap between the *Max Mean SNR* scheme and the proposed *Max LB Mean SNR* scheme increases slightly for higher values of θ and μ. This may be attributed to the fact that the third term (ignored for lower bounding the SNR) in

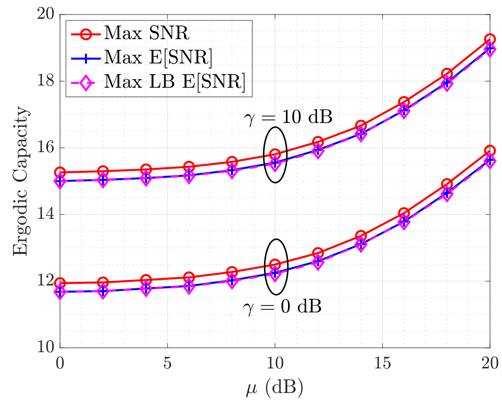

Figure 4. Ergodic capacity with respect to μ.

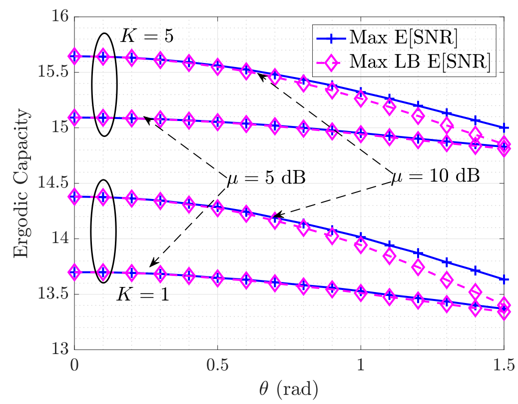

Figure 5. Ergodic Capacity vs. the difference of departure angles indirect and direct links.

(17) becomes unavoidable. Despite this observation, it is worth noting that the gap is very small.

V. Conclusion

This paper proposes a statistical CSI-based optimal beamforming scheme for maximizing the mean SNR of a RIS-aided MISO communication system when both direct and indirect links follow Rician fading. Unlike prior works where such problems are often tackled algorithmically, we derived closed-form expressions of optimal transmit beamformer and the optimal RIS phase shift matrix that maximize a tight lower bound on mean SNR. To characterize the performance of the proposed scheme, we derive its achievable outage probability and ergodic capacity. In particular, we show that the effective channel envelope approximately follows Rice distribution which we consequently used to derive approximate expressions for outage and ergodic capacity that are tight. Using numerical comparisons, we demonstrate that the derived outage expression acts as a tight upper bound for the exact mean SNR maximization-based scheme. Likewise, the achievable capacity of the proposed scheme is shown to be a close lower bound.

Appendix

Let us define $\xi_1 = \boldsymbol{\psi}^{\star T}\text{diag}(\mathbf{h})\mathbf{H}\mathbf{f}^\star$ and $\xi_2 = \mathbf{g}^T\mathbf{f}^\star$ and rewrite SNR given in (4) as

$$\gamma|\boldsymbol{\psi}^{\star T}\text{diag}(\mathbf{h})\mathbf{H}\mathbf{f}^\star + \mu\mathbf{g}^{\mathrm{T}}\mathbf{f}^\star|^2 = \gamma|\xi_1 + \mu\xi_2|^2,$$

Thus, outage can be evaluated as

$$\mathrm{P}_{\mathrm{out}}(\beta) = \mathbb{P}[|\xi_1 + \mu\xi_2| \leq \sqrt{\beta/\gamma}]. \tag{25}$$

Using channel models from (1) and (2), we obtain

$$\xi_1 = \kappa_l^2 a_1 + \kappa_l \kappa_n a_2 + \kappa_l \kappa_n a_3 + \kappa_n^2 a_4, \tag{26}$$

$$\xi_2 = \kappa_l b_1 + \kappa_n b_2, \tag{27}$$

where $a_1 = \boldsymbol{\psi}^{\star T}\mathrm{diag}(\bar{\mathbf{h}})\bar{\mathbf{H}}\mathbf{f}^\star$, $a_2 = \boldsymbol{\psi}^{\star T}\mathrm{diag}(\bar{\mathbf{h}})\tilde{\mathbf{H}}\mathbf{f}^\star$, $a_3 = \boldsymbol{\psi}^{\star T}\mathrm{diag}(\tilde{\mathbf{h}})\bar{\mathbf{H}}\mathbf{f}^\star$, $a_4 = \boldsymbol{\psi}^{\star T}\mathrm{diag}(\tilde{\mathbf{h}})\tilde{\mathbf{H}}\mathbf{f}^\star$, $b_1 = \bar{\mathbf{g}}^T\mathbf{f}^\star$, $b_2 = \tilde{\mathbf{g}}^T\mathbf{f}^\star$.

We now find distributions of $\tilde{\mathbf{p}} = \boldsymbol{\psi}^\star\mathrm{diag}(\tilde{\mathbf{h}})$, $\tilde{\mathbf{q}} = \tilde{\mathbf{H}}\mathbf{f}^\star$, and $\tilde{u} = \tilde{\mathbf{g}}^T\mathbf{f}^\star$. These results will be used to identify the distributions of a_is and b_is, which subsequently will be employed to obtain the distributions of the channel envelope and SNR. Using the rotational invariance property of zero-mean complex Gaussian distribution, we obtain $\tilde{\mathbf{p}} \sim \mathcal{CN}(0, \mathrm{I_N})$. Further, by using $\|\mathbf{f}^\star\|^2 = 1$, and the linear combination property of zero-mean complex Gaussian random variable, we find that $\tilde{\mathbf{q}} \sim \mathcal{CN}(0, \mathrm{I_N})$ and $\tilde{u} \sim \mathcal{CN}(0, 1)$.

Terms a_1 and b_1: The terms a_1 and b_1 are constants as given above. The term a_1 can be simplified as

$$a_1 = \frac{N|\mathbf{e}_n\mathbf{f}^\star|}{|\bar{\mathbf{g}}^T\mathbf{f}^\star|}\bar{\mathbf{g}}^T\mathbf{f}^\star. \tag{28}$$

Term a_2: Since $\mathbf{p} = \boldsymbol{\psi}^{\star T}\mathrm{diag}(\bar{\mathbf{h}})$ is a complex vector of unit-magnitude elements, we can show that $a_2 = \mathbf{p}\tilde{\mathbf{q}}$ is a zero-mean complex Gaussian random variable with variance

$$\mathrm{Var}[a_2] = \mathbb{E}[\mathbf{p}\tilde{\mathbf{q}}\tilde{\mathbf{q}}^H\mathbf{p}^H] = \mathbf{p}\mathbb{E}[\tilde{\mathbf{q}}\tilde{\mathbf{q}}^H]\mathbf{p}^H = \mathbf{p}\mathbf{p}^H = N.$$

Term b_2: Note $b_2 = \tilde{u}$ is a zero-mean unit variance complex Gaussian, as mentioned above.

Term a_3: With $\mathbf{q} = \bar{\mathbf{H}}\mathbf{f}^\star$, we can show that $a_3 = \tilde{\mathbf{p}}\mathbf{q}$ is also a zero-mean complex Gaussian with variance

$$\mathrm{Var}[a_3] = \mathbb{E}[\mathbf{q}^H\tilde{\mathbf{p}}^H\tilde{\mathbf{p}}\mathbf{q}] = \mathbf{q}^H\mathbb{E}[\tilde{\mathbf{p}}^H\tilde{\mathbf{p}}]\mathbf{q} = \mathbf{q}^H\mathbf{q} = \|\bar{\mathbf{H}}\mathbf{f}^\star\|^2.$$

Term a_4: Further, we can show that $a_4 = \tilde{\mathbf{p}}\tilde{\mathbf{q}}$ approximately follows the complex Gaussian as it is the sum of the product of two Gaussian variables. The mean of a_4 is zero, and its variance is

$$\begin{aligned}\mathbb{E}[a_4^H a_4] &= \mathbb{E}[\tilde{\mathbf{q}}^H\tilde{\mathbf{p}}^H\tilde{\mathbf{p}}\tilde{\mathbf{q}}],\\ &= \mathbb{E}[\tilde{\mathbf{q}}^H\mathbb{E}[\tilde{\mathbf{p}}^H\tilde{\mathbf{p}}]\tilde{\mathbf{q}}],\\ &= \mathbb{E}[\tilde{\mathbf{q}}^H\tilde{\mathbf{q}}],\\ &= \sum\nolimits_{n=0}^{N-1}\mathbf{E}[|\tilde{\mathbf{q}}_n|^2],\\ &= N.\end{aligned}$$

Distribution of ξ_1 and ξ_2: Compiling the above results gives the distributions of ξ_1 (26) (approximate) and ξ_2 (27) as

$$\xi_1 \sim \mathcal{CN}\left(\kappa_l^2\frac{N|\mathbf{e}_n\mathbf{f}^\star|}{|\bar{\mathbf{g}}^T\mathbf{f}^\star|}\bar{\mathbf{g}}^T\mathbf{f}^\star, N\kappa_n^2(1 + \kappa_l^2|\mathbf{e}_n\mathbf{f}^\star|^2)\right),$$

$$\xi_2 \sim \mathcal{CN}\left(\kappa_l\bar{\mathbf{g}}^T\mathbf{f}^\star, \kappa_n^2\right).$$

Thus, we obtain $\xi_1 + \mu\xi_2 \sim \mathcal{CN}(m, \sigma^2)$ (approximately), where

$$m = \kappa_l^2\frac{N|\mathbf{e}_n\mathbf{f}^\star|}{|\bar{\mathbf{g}}^T\mathbf{f}^\star|}\bar{\mathbf{g}}^T\mathbf{f}^\star + \mu\kappa_l\bar{\mathbf{g}}^T\mathbf{f}^\star,$$

and $\sigma^2 = N\kappa_n^2(1 + \kappa_l^2|\mathbf{e}_n\mathbf{f}^\star|^2) + \mu^2\kappa_n^2$.

Channel envelope distribution: We note that the magnitude of a nonzero-mean complex Gaussian follows the Rice distribution. Hence, we conclude that $|\xi_1 + \mu\xi_2|$ is approximately Rice distributed, i.e.,

$$|\xi_1 + \mu\xi_2| \sim \mathrm{Rice}(\nu, \sigma/\sqrt{2}),$$

where $\nu = |m|$. Finally, using (25) and the CDF of Rice distribution, the outage probability is obtained as in (23).

References

[1] K. K. Kota, M. S. S. Manasa, P. D. Mankar, and H. S. Dhillon, "Statistically optimal beamforming and ergodic capacity for RIS-aided MISO systems," *IEEE Access*, vol. 12, pp. 10 699–10 717, 2024.

[2] C. Pan, H. Ren, K. Wang, J. F. Kolb, M. Elkashlan, M. Chen, M. Di Renzo, Y. Hao, J. Wang, A. L. Swindlehurst, X. You, and L. Hanzo, "Reconfigurable intelligent surfaces for 6G systems: Principles, applications, and research directions," *IEEE Commun. Mag.*, vol. 59, no. 6, pp. 14–20, 2021.

[3] E. Björnson, H. Wymeersch, B. Matthiesen, P. Popovski, L. Sanguinetti, and E. de Carvalho, "Reconfigurable intelligent surfaces: A signal processing perspective with wireless applications," *IEEE Sig. Processing Mag.*, vol. 39, no. 2, pp. 135–158, 2022.

[4] T. J. Cui, M. Q. Qi, X. Wan, J. Zhao, and Q. Cheng, "Coding metamaterials, digital metamaterials and programmable metamaterials," *Light: Science & Applications*, vol. 3, no. 10, pp. e218–e218, 2014.

[5] M. Di Renzo, K. Ntontin, J. Song, F. H. Danufane, X. Qian, F. Lazarakis, J. De Rosny, D.-T. Phan-Huy, O. Simeone, R. Zhang *et al.*, "Reconfigurable intelligent surfaces vs. relaying: Differences, similarities, and performance comparison," *IEEE Open Journal of the Communications Society*, vol. 1, pp. 798–807, 2020.

[6] B. Zheng, C. You, W. Mei, and R. Zhang, "A survey on channel estimation and practical passive beamforming design for intelligent reflecting surface aided wireless communications," *IEEE Commun. Surveys Tuts.*, vol. 24, no. 2, pp. 1035–1071, 2022.

[7] M. Dajer, Z. Ma, L. Piazzi, N. Prasad, X.-F. Qi, B. Sheen, J. Yang, and G. Yue, "Reconfigurable intelligent surface: design the channel – A new opportunity for future wireless networks," *Dig. Commun. Net*, vol. 8, no. 2, pp. 87–104, 2022.

[8] X. Yu, D. Xu, and R. Schober, "MISO wireless communication systems via intelligent reflecting surfaces," in *IEEE ICCC*, 2019, pp. 735–740.

[9] ——, "Optimal beamforming for MISO communications via intelligent reflecting surfaces," in *IEEE SPAWC*, 2020.

[10] B. Ning, Z. Chen, W. Chen, and J. Fang, "Beamforming optimization for intelligent reflecting surface assisted MIMO: A sum-path-gain maximization approach," *IEEE Wireless Commun. Lett.*, vol. 9, no. 7, pp. 1105–1109, 2020.

[11] H. Zhang, S. Ma, Z. Shi, X. Zhao, and G. Yang, "Sum-rate maximization of RIS-aided multi-user MIMO systems with statistical CSI," *IEEE Trans. Wireless Commun.*, 2022.

[12] C. Luo, X. Li, S. Jin, and Y. Chen, "Reconfigurable intelligent surface-assisted multi-cell MISO communication systems exploiting statistical CSI," *IEEE Wireless Communications Letters*, vol. 10, no. 10, pp. 2313–2317, 2021.

[13] K. Zhi, C. Pan, H. Ren, and K. Wang, "Statistical CSI-based design for reconfigurable intelligent surface-aided massive MIMO systems with direct links," *IEEE Wireless Commun. Lett.*, vol. 10, no. 5, pp. 1128–1132, 2021.

[14] X. Hu, J. Wang, and C. Zhong, "Statistical CSI based design for intelligent reflecting surface assisted MISO systems," *Science China Information Sciences*, vol. 63, pp. 1–10, 2020.

[15] P. Xu, W. Niu, G. Chen, Y. Li, and Y. Li, "Performance analysis of RIS-assisted systems with statistical channel state information," *IEEE Trans. Veh. Technol.*, vol. 71, no. 1, pp. 1089–1094, 2022.

[16] A. M. Salhab and M. H. Samuh, "Accurate performance analysis of reconfigurable intelligent surfaces over Rician fading channels," *IEEE Wireless Commun. Lett.*, vol. 10, no. 5, pp. 1051–1055, 2021.

[17] W. Tang, M. Z. Chen, X. Chen, J. Y. Dai, Y. Han, M. Di Renzo, Y. Zeng, S. Jin, Q. Cheng, and T. J. Cui, "Wireless communications with reconfigurable intelligent surface: Path loss modeling and experimental measurement," *IEEE Trans. Wireless Commun*, vol. 20, no. 1, pp. 421–439, 2020.